The Many Faces of Supernova Remnants

Tea Temim, Brian J. Williams and Laura Lopez

Supernova (SN) explosions are among the most energetic events in the Universe and play a significant role in virtually all aspects of astrophysics, from studies of meteorites to modern day cosmology. The remnants they leave behind shape the dynamics and chemical evolution of galaxies. The tremendous energy ($\sim 10^{51}$ ergs) they release into the interstellar medium (ISM) significantly affects the distribution and thermal state of gas and dust, while their ejecta enrich the chemical content of interstellar clouds that form new generations of stars. They are also sites of particle acceleration, and likely the primary sources of Galactic cosmic rays.

The X-ray signatures of supernova remnants (SNRs) arise from several sources, including the hot plasmas produced by SN shocks, line emission from collisionally excited ions and radioactive elements, and synchrotron emission from particles accelerated in shocks and pulsar winds (see Fig. 1 for a typical SNR spectrum). Consequently, X-ray observations of SNRs carried out in the last decades have served as essential probes of the physical conditions and processes that characterize these objects. X-ray imaging spectroscopy with *Chandra* in particular has helped revolutionize our understanding of SNRs of both Type Ia and core collapse (CC) explosions.

The importance of Type Ia SNe in astrophysics is well-established, particularly in light of the 2011 Nobel Prize in Physics awarded for the observations of these SNe in distant galaxies that led to the discovery of dark energy. Despite detailed study of these important objects, there is significant debate over whether Type Ia SNe result from single-degenerate (the explosion of a white dwarf that has accreted matter from a non-degenerate companion) or double-degenerate systems (the merger of two

sub-Chandrasekhar mass white dwarfs). The general consensus in the literature is that most Type Ia SNe result from the double-degenerate model; Gilfanov & Bogdan (2010) used *Chandra* observations of the X-ray luminosities of several nearby galaxies to place an upper limit on the number of accreting white dwarf systems, concluding that the single-degenerate channel accounts for no more than 5% of all SNe Ia. Another open issue is the nature of the explosion itself. The location and propagation of the nuclear burning front, the nucleosynthetic products of the burning, and the distribution of the ejecta after the explosion are all areas of active study via theory, computation, and observation. These issues can all be probed through studies of remnants of Type Ia SNe.

CC SNe follow the gravitational collapse of a massive ($> 8 M_\odot$) star. They are relatively common phenomena across the Universe, occurring a few times per century in a "normal" galaxy. Among the roughly 300 known SNRs in our own Milky Way, the majority are thought to originate from CC events.
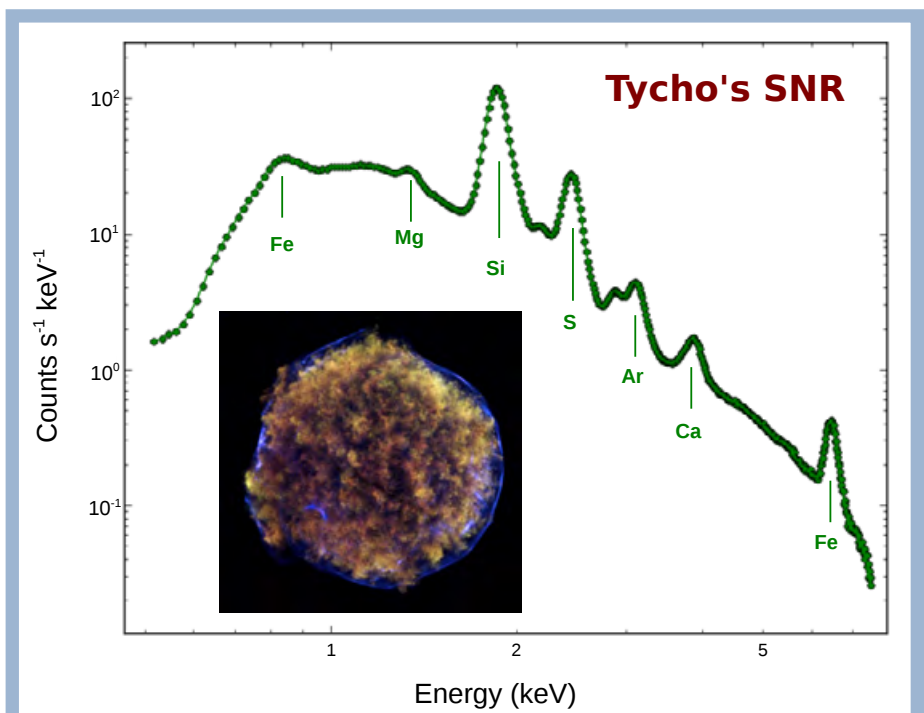

Fig. 1 — Chandra spectrum and press release image of Tycho's SNR. The example represents a typical SNR X-ray spectrum with three main emission mechanisms at work: thermal bremsstrahlung and line emission from the shocked gas at a temperature of ~ 1 keV (red/green colors in the image), and nonthermal synchrotron continuum from relativistic electrons that dominates above ~ 3 keV (blue color in the image). The absorbing column density is < 10^{22} cm^{-2}. Note: North is up and East to the left in all shown images. Press release image credit: NASA/CXC/Chinese Academy of Sciences/F. Lu et al.

Since its first-light image of Cassiopeia A, *Chandra* has revealed that CC SNRs are complex and diverse sources. *Chandra*'s exquisite imaging and sensitivity fostered the discovery of previously unknown neutron stars within several CC SNRs. Furthermore, *Chandra*'s spatially resolved spectroscopic capabilities have enabled detailed studies of the temperature, composition, and ionization state of shocked gas across remnants. The emerging picture is that the hydrodynamical evolution of CC SNRs can vary substantially depending on several factors, including the presence of neutron stars or pulsars, the asymmetries inherent to the explosions, and the structure of the surrounding circumstellar medium (CSM).

In this article, we highlight recent *Chandra* studies of well known Type Ia SNRs, and studies of three classes of CC SNRs whose evolution deviates from the prototypical example of a spherical SN in a homogeneous medium, SNRs that: interact with nearby molecular clouds, originate from bipolar/jet-driven explosions, and contain an energetic pulsar generating a synchrotron-emitting wind of relativistic particles.

Circumstellar Interactions & Asymmetric Explosions in Type Ia SNRs

Much of the recent work by *Chandra* on the remnants of Type Ia SNe has focused on exploring the issues of their origin from the point of view of the interaction of the expanding SN blast wave with its surroundings, or the distribution and composition of the ejecta. *Chandra*'s sharp resolution allows both spatially-resolved spectroscopy on small scales and the detection of proper motions of young SNRs expanding over timescales accessible to the 15+ year lifetime of the mission.

Kepler's SNR has drawn considerable attention in recent years. The remains of the SN of 1604 A.D. (as a note, also the last historically observed Galactic SN), Kepler is ~ 3.5′ in diameter, making it an ideal target for the high angular resolution of *Chandra*. A recent *Chandra* press release image is shown in Fig. 2. The origin of Kepler had long been debatable, though work with *Chandra* and other observatories has established it reasonably firmly in the SN Ia category. However, unlike most SN Ia remnants that expand into the undisturbed ISM (Badenes et al. 2007), Kepler is interacting with a dense CSM that seems to have resulted from pre-SN mass

loss from the progenitor system (Reynolds et al. 2007, Williams et al. 2012). Kepler was the first example of the remnant of a SN Ia that is interacting with a dense CSM wind.

Hydrodynamic (HD) simulations by Burkey et al. (2013) showed that the morphology of Kepler is consistent with the blast wave from the SN encountering an equatorial wind from a companion that is an evolved asymptotic giant branch (AGB) star (i.e., a single-degenerate origin). This work also decomposed a deep (750 ks) *Chandra* observation into various spectral components on small scales, showing the spatial location of different ejecta species in the remnant, as well as the portions dominated by CSM interaction. Additionally, Patnaude et al. (2012) used HD simulations and X-ray spectral modeling to conclude that Kepler may have resulted from an overluminous SN Ia that produced roughly a solar mass of Ni, and that the explosion took place within a slow, dense CSM wind with a small central cavity. On the other hand, Chiotellis et al. (2012) argue that Kepler resulted from a sub-energetic Type Ia SN. Their models also
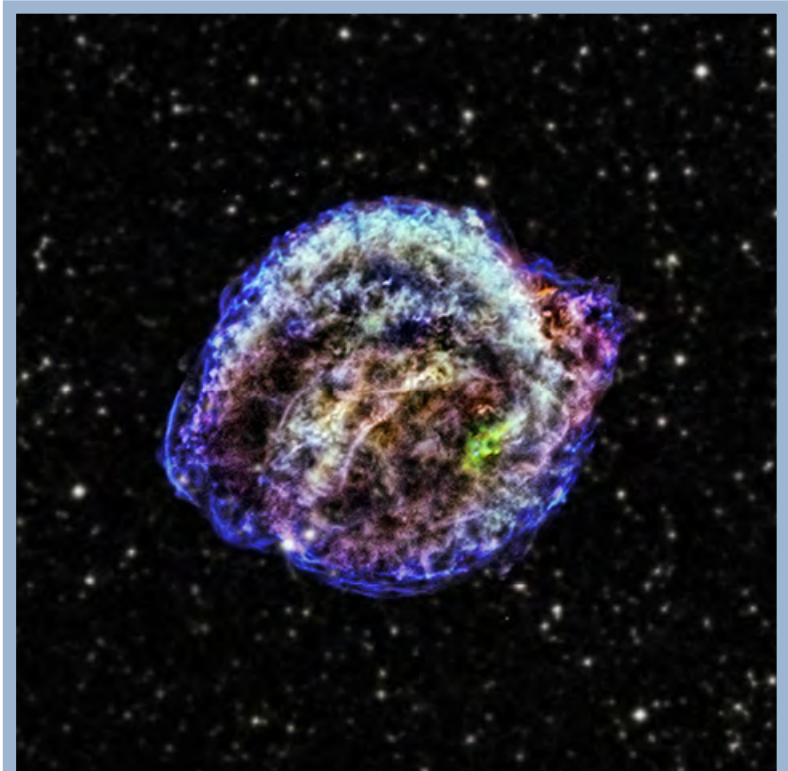

Fig. 2 — Chandra press release image of Kepler's SNR. Red, green, and blue correspond to soft, medium, and hard X-rays, respectively. An optical Digital Sky Survey (DSS) image is used as the background. There is strong evidence for a dense CSM in Kepler, implying a single-degenerate origin (see text for details). Credit: NASA/CXC/NCSU/M. Burkey et al.

require the presence of a dense CSM, generated by the winds from a symbiotic binary consisting of a white dwarf and an AGB companion. Clearly, Kepler and Kepler-like SNRs are deserving of more study to determine their origins.

The remnant of SN 1006 A.D. provides something of a contrast to Kepler. There, the densities are extremely low with no indication of a CSM, making a double-degenerate progenitor system seem more likely. Perhaps the most *Chandra*-centric result from SN 1006 is a study of the proper motions of the forward shock, which moves at a rate of roughly one *Chandra* pixel per year. Fig. 3 shows a difference image in two epochs (2003 and 2012) of *Chandra* observations of SN 1006 (Winkler et al. 2014). Expansion along the NE and SW limbs, where the emission is dominated by non-thermal synchrotron X-rays, is readily apparent, as the shocks there move at 5000–6000 km s^{-1}. The ISM density is somewhat higher in the NW, where X-rays are dominated by thermal emission from the shocked ISM. Proper motions there are less apparent but still visible. The shock speed there is significantly slower, moving at $\sim$ 3000 km s^{-1} (Katsuda et al. 2013). That SN 1006 is still approximately circular, despite such variations in the expansion rate, indicates that the blast wave's interaction with the denser material in the NW is a relatively recent phenomenon. Winkler et al. (2013) estimate that this interaction began about 150 years ago.

Perhaps the most interesting new result on SN 1006 is the discovery that the ejecta distribution is asymmetric. Equivalent width image maps of the various atomic species present in the thermal X-ray plasma can map out the distribution of these elements within the remnant. *Chandra* maps from Winkler et al. (2014) and *Suzaku* maps from Uchida et al. (2013) both show that Si and Fe, primarily originating from the reverse-shocked ejecta, are more prevalent in the SE portion of SN 1006. O and Ne, on the other hand, which likely originate from the forward-shocked ISM, are more uniformly distributed. HD models of SNe Ia can show asymmetries in the ejecta related to the particulars of the explosion; see, for example, Seitenzahl et al. (2013).

Further evidence for an asymmetric explosion of a (likely) SN Ia is found in G1.9+0.3, the youngest known remnant in the Galaxy at an age of about 150 years. The young age of this remnant was first discovered by Reynolds et al. (2008), who compared a newly obtained *Chandra* image to an archival radio
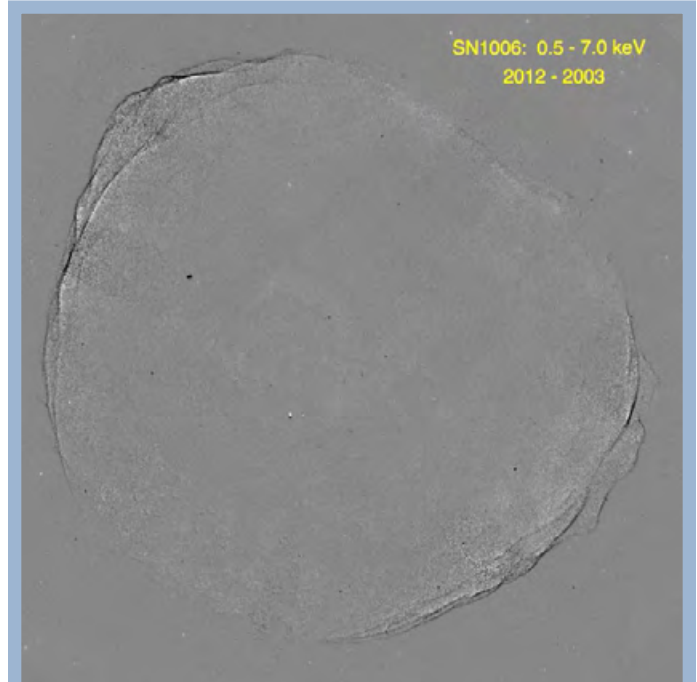

Fig. 3 — Difference image between the 2003 and 2012 Chandra observations of SN 1006, showing expansion of the remnant during that time period (Fig. 6 from Winkler et al. 2014). Expansion is particularly evident along the synchrotron-dominated NE and SW limbs, where shock speeds are 5000–6000 km s^{-1}. Image is approximately 40′ on a side.

image from two decades prior, noting that the remnant had expanded by roughly 20% during that time. In G1.9+0.3, the intermediate mass elements Si and S, byproducts of O-burning, have a different spatial distribution than Fe (Borkowski et al. 2013). Ejecta velocities in this remnant are observed to be > 18,000 km s^{-1}, which may imply an energetic Type Ia event. The expansion velocities of the forward and reverse shocks in G1.9+0.3 also show significant variation by factors of $\sim$ 60% in different places in the remnant (Borkowski et al. 2014), again indicating an asymmetric explosion.

Chandra observations of Tycho's SNR, the remnant of the SN of 1572 A.D., show remarkable differences when viewed in soft and hard X-rays. At lower energies, below $\sim$ 2 keV, the X-ray emission is dominated by thermal emission from the ejecta, mostly Si, in a somewhat fluffy morphology (see Fig. 1). At hard X-ray energies, emission is dominated by nonthermal synchrotron photons, mostly coming from the forward shock. However, in the western portion, a curious pattern emerges of stripes emanating radially outwards. This pattern has not yet been seen in any other remnant. Eriksen et al. (2011) argue that these stripes are

regions of unusually high magnetic field turbulence, and their roughly constant spacing corresponds to the gyroradii of $10^{14}-10^{15}$ eV protons. If this interpretation is correct, it would be evidence of the acceleration of protons by SNR shocks, long thought to be the source of most Galactic cosmic rays, at least up to energies of around 10^{15} eV.

Shocked Clouds & Enriching Jets in Core-Collapse SNRs

Since the progenitors of CC SNe have short main-sequence lives, the explosions tend to occur within the dense medium from which the massive stars were born. Consequently, a common trait of CC SNRs is interaction with an inhomogeneous or dense CSM. In fact, roughly one quarter of all Galactic SNRs show evidence of interaction with molecular clouds, such as the coincidence of OH masers (which indicate the presence of shocked molecular gas: e.g., Wardle & Yusef-Zadeh 2002).

The SNR-molecular cloud interaction has a profound influence on the X-ray morphologies and spectra of the SNRs. Large-scale density gradients can result in substantial deviations from spherical symmetry (e.g., Lopez et al. 2009). Additionally, a large number of interacting SNRs have centrally dominated, thermal X-ray emission, whereas their radio morphologies are shell-like. Known as mixed morphology (MM) SNRs, ~ 40 of these sources have been identified in the Milky Way (Vink 2012). Based on observations with *Chandra* and other modern X-ray facilities, MM SNRs can have enhanced metal abundances (Lazendic

& Slane 2006) and/or isothermal plasmas across their interiors.

In the past decade or so, astronomers have realized that many MM SNRs also have "overionized" plasmas. Typically in young SNRs, shocks create ionizing plasmas which slowly reach collisional ionization equilibrium (CIE). However, X-ray observations with ASCA first revealed possible evidence for overionization in SNRs, where the electron temperature kT_e derived from the bremsstrahlung continuum is systematically lower than the effective ionization temperature kT_z given by the line ratios (Kawasaki et al. 2003, 2005). The comparison of *Chandra* X-ray spectra from a CIE plasma and from an overionized plasma is shown in Fig. 4. Additionally, recent observations with *Suzaku* have discovered the presence of radiative recombination continuum features in these SNRs, conclusive evidence of overionization (e.g., Yamaguchi et al. 2009, Ozawa et al. 2009).

In a collisional plasma (as in SNRs), overionized plasma is one signature of rapid electron cooling, and the physical origin of this cooling in SNRs remains a topic of debate. One scenario where cooling can occur is thermal conduction, in which the hot ejecta in the SNR interior may cool by efficiently exchanging heat with the exterior material (e.g., Cox et al. 1999). Alternatively, the cooling may take place through adiabatic expansion, where the SN blast wave expands through dense CSM into a rarefied ISM (e.g., Itoh & Masai 1989). Localization of the overionized plasma is critical to ascertain the cooling scenario responsible for the overionization. Recently, Lopez et al. (2013a) used *Chandra* data to map the overionized plasma in W49B. Specifically, they undertook a spatially resolved spectroscopic analysis and compared kT_e derived by modeling the continuum to kT_z measured from the flux ratio of He-like to H-like lines. As the overionization was concentrated in the west, where the ejecta are expanding unimpeded, it was concluded that adiabatic expansion of the hot plasma is likely to be the dominant cooling mechanism.

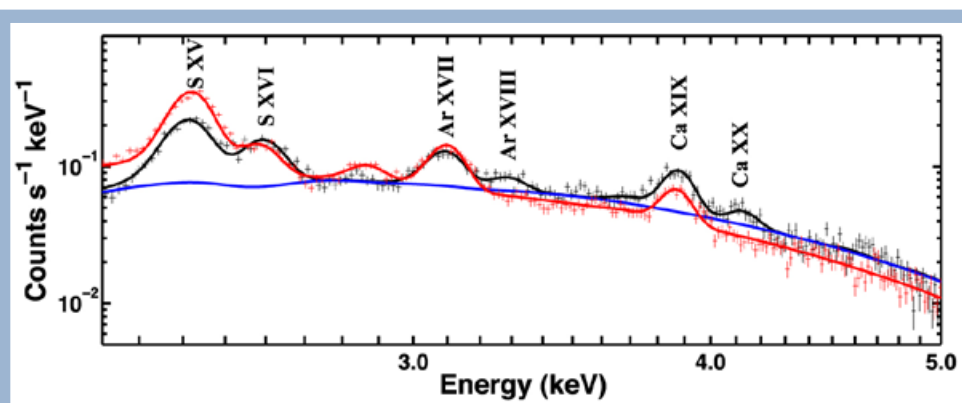In the past few decades, evidence has mounted that SNe can

Fig. 4 — Example Chandra spectra from a collisional ionization equilibrium (CIE) plasma and from an overionized plasma. The black line shows the observed overionized data from the SNR W49B, and the red line is for synthetic data if the plasma was in CIE. The blue line shows the model of the continuum. In this case, the CIE plasma spectrum has substantially greater S XV flux and no discernible Ar XVIII or Ca XX. (Figure is adapted from Lopez et al. 2013a).
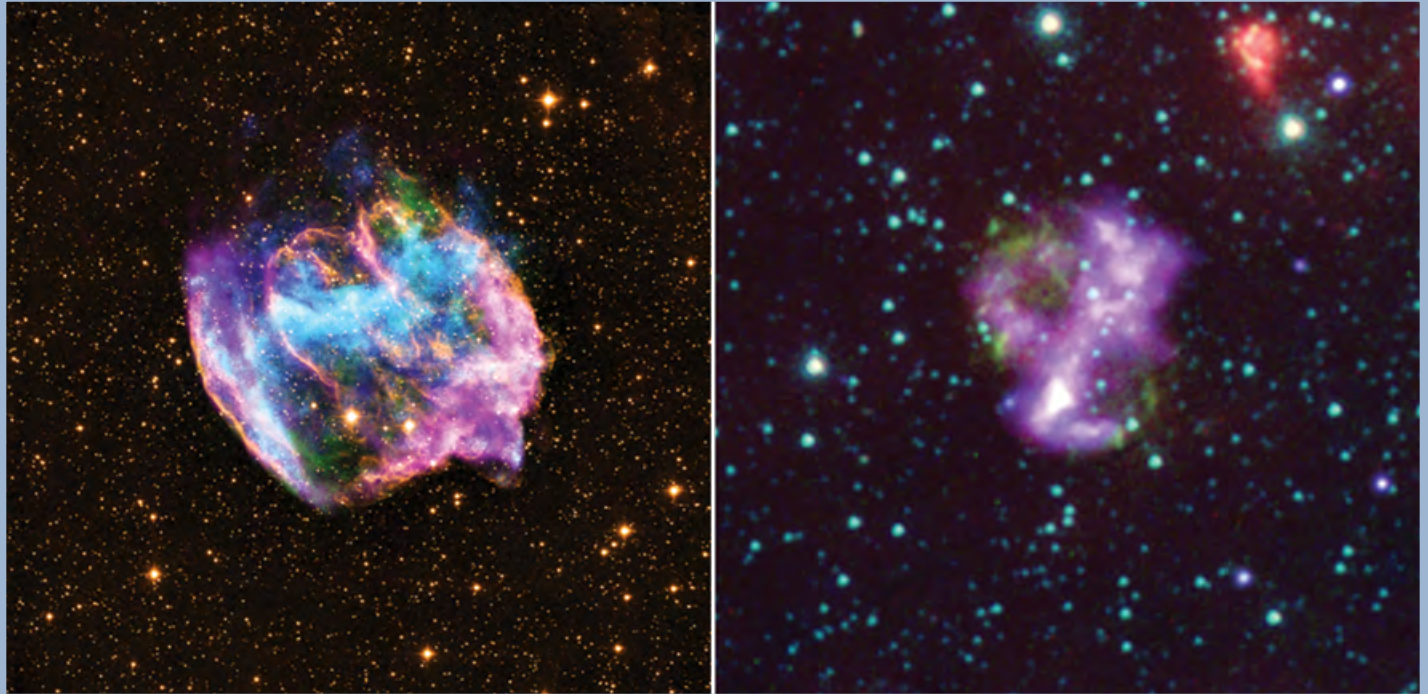
Fig. 5 — Mulitwavelength images of two elliptical SNRs thought to be from bipolar/jet-driven explosions (Lopez et al. 2013b, 2014). Left: SNR W49B, with Chandra X-rays in blue, IR (Palomar) in yellow, and radio (NSF/NRAO/VLA) in purple. Right: SNR 0104−72.3, with Chandra X-rays in purple and IR (NASA/JPL-Caltech) in red, green, and blue.

have significant deviations from spherical symmetry. In particular, spectropolarimetry studies demonstrate that both Type Ia and CC SNe are aspherical near maximum brightness (e.g., Wang & Wheeler 2008). SNRs retain imprints of the geometry of their progenitors' explosions, and spectro-imaging studies with *Chandra* have revealed marked asymmetries in young SNRs, such as the silicon-rich "jet" in Cassiopeia A which protrudes from the remnant's forward shock (Hughes et al. 2000). The analysis of the morphology of the *Chandra* X-ray line emission in Galactic and Large Magellanic Cloud SNRs established that CC SNRs are statistically more asymmetric and elliptical than Type Ia SNRs (Lopez et al. 2009, 2011). Infrared observations of SNRs were later shown to display these same properties (Peters et al. 2013).

Asymmetric explosions also alter the nucleosynthetic yields of the SNe (e.g., Maeda & Nomoto 2003). For example, while spherical CC events are predicted to produce $\sim 0.07 - 0.15$ M$_\odot$ of ^{56}Ni, bipolar/jet-driven CC SNe (with increased kinetic energy at the poles of exploding stars) can have 5–10 times more nickel (Umeda & Nomoto 2008).

Bipolar/jet-driven CC SNe are thought to occur among $\sim 1-2\%$ of Type Ib/Ic SNe (Soderberg et al.

2010), and some fraction of these events are associated with long-duration gamma-ray bursts (GRBs; e.g., Izzard et al. 2004). As GRBs are typically detected at cosmological distances, identification of local analogues among the nearby SNR population would be useful to constrain the physics, dynamics, and nucleosynthesis of these explosions (e.g., Ramirez-Ruiz & MacFadyen 2010). Based on the rates of bipolar/jet-driven explosions observed in external galaxies, it is reasonable to expect a few bipolar/jet-driven CC SNRs among the several hundred known in the Local Group. Recently, two possible bipolar/jet-driven CC SNRs have been identified based on *Chandra* X-ray observations (see Fig. 5): SNR W49B in the Milky Way and SNR 0104−72.3 in the Small Magellanic Cloud (SMC). Several lines of evidence support a bipolar origin for these SNRs, including their *Chandra* X-ray morphologies, the chemical abundances derived from *Chandra* spectra, and the star-formation histories in their vicinities (Lopez et al. 2013b, 2014). The identification of a bipolar SNR in the SMC (a low metallicity galaxy) is consistent with recent work which shows that bipolar/jet-driven SNe prefer low-metallicity environments (e.g., Fruchter et al. 2006, Sanders et al. 2012).

Fleeing Pulsars & Crushed Winds in Composite SNRs

Composite SNRs are a special subclass of CC remnants that are not only characterized by forward and reverse shocks that expand into the ambient medium and the cold SN ejecta, but also a highly magnetic, rapidly rotating pulsar that converts its spin-down energy into a wind of relativistic particles. The acceleration of these particles in the pulsar's magnetic field produces a synchrotron-emitting pulsar wind nebula (PWN) that retains a torus and jet morphology imprinted by the rotating magnetic field. In composite SNRs, the evolution of the PWN is coupled to the evolution of its host SNR. The complex interaction that occurs allows us to probe the properties of the pulsar, the SN ejecta, the progenitor star, and the structure of the ambient medium. It also alters the relativistic particle population that eventually escapes into the ISM, and gives rise to an excess of low-energy particles that produce γ-ray emission through inverse-Compton scattering (e.g., Abdo et al. 2012, Slane et al. 2010). For these reasons, the study of the composite class of SNRs has been of particular interest.
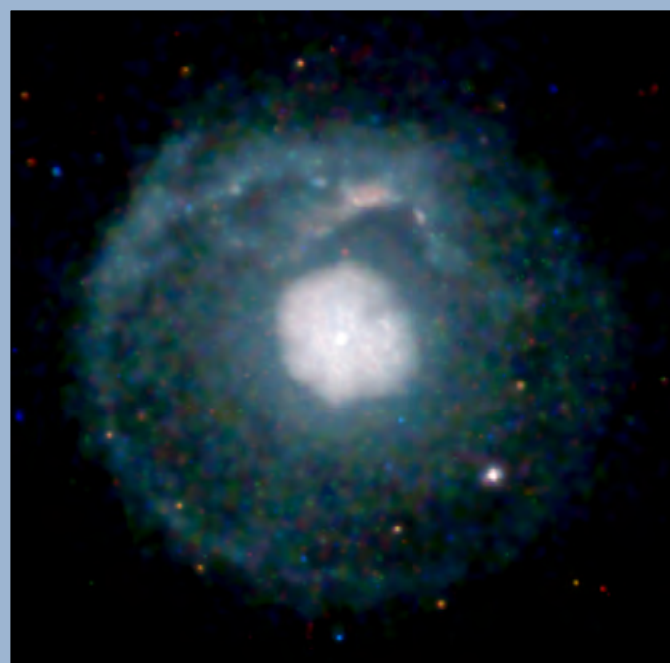

Fig. 6 — Chandra press release image of the young composite SNR G21.5-0.9 (Matheson & Safi-Harb 2010) whose PWN is expanding into the cold SN ejecta, yet to be reached by the SN reverse shock. The surrounding faint X-ray shell originates from a dust scattering halo and synchrotron emission from particles accelerated by the forward shock. The 0.2–1.5 keV band is shown in red, 1.5–3 keV in green, and 3–10 keV in blue.

Chandra observations of composite SNRs in various stages of evolution significantly advanced our understanding of these systems. While the basic picture of their evolution was generally understood, *Chandra* filled in the crucial details pertaining to the transitional phases of evolution. High-resolution imaging provided unprecedentedly detailed views of the structures that form in each stage of development, from the well-defined tori and jets in younger system to highly disrupted nebulae in older ones. Spectral studies revealed the spatially varying spectra of the evolving particle population injected by the pulsar, and provided evidence for the mixing of SN ejecta with PWN material. Here, we highlight only a selection of studies of the PWN/SNR interaction conducted with *Chandra* in recent years.

The PWNe in very young composite SNRs are still driving a shock into the cold SN ejecta that have not been heated by the reverse shock, and tend to be located close to the centers of their host SNRs. Well known examples of systems at this early stage of evolution include G21.5-0.9 and G11.2-0.3. The PWN in G11.2-0.3, powered by a 65 ms pulsar, is located near the geometric center of a highly symmetric, circular SNR shell (Kaspi et al. 2001, Roberts et al. 2003). Considering that typical pulsar kick velocities are on the order of a few hundred km s^{-1}, the pulsar's proximity to its birthplace suggests that the system is young. SNR G21.5-0.9 is another young system that shows a circular PWN (Fig. 6), embedded in a more extended halo of fainter X-ray emission (Slane et al. 2000, Safi-Harb et al. 2001). The inner core of the PWN is extended in X-rays, indicating a possible torus structure around the pulsar. The diffuse shell of X-ray emission is attributed to a dust scattering halo, and the outer brightened limb to nonthermal emission from particles accelerated by a very fast forward shock (Bocchino et al. 2005, Matheson & Safi-Harb 2012). All these properties are consistent with a very young SNR age of < 1000 yr, whose PWN drives a shock into the cold SN ejecta. This is further supported by the discovery of [Fe II] 1.64 µm emission that traces the outer edge of the PWN (Zajczyk et al. 2012).

As a composite SNR evolves, the reverse shock propagates into its interior and eventually reaches the boundary of the expanding PWN at timescales of a few thousand years. *Chandra* observations of the oxygen-rich SNR G292.0+1.8 revealed torus and jet structures, embedded in a more extended nebula (Hughes et al. 2001, Park et al. 2007). The coinciding position of the outer boundary of the PWN with the SN reverse shock, as revealed by radio and *Chandra* HETGS observations, suggests that G292.0+1.8 is in a special

stage of evolution when the reverse shock is just beginning to interact with the PWN (Gaensler & Wallace 2003, Bhalerao et al. 2015). MSH 11-62, shown in Fig. 7, is another SNR whose PWN's asymmetric morphology suggests that it has been compressed by the reverse shock (Slane et al. 2012).

The next stage of a composite SNR's evolution becomes significantly more complicated. The reverse shock collision drastically modifies the evolution of the PWN and its observational signatures. Since the density of the ambient medium into which the SNR expands is typically non-uniform, the resulting reverse shock often propagates asymmetrically, arriving faster from the direction of the higher ambient density. This, along with any offset of the PWN due to the pulsar's kick velocity (typically several hundreds of km s^{-1}), causes the reverse shock to crush the PWN asymmetrically and gives rise to complex structures and mixing of the SN ejecta with PWN material (Blondin et al. 2001, van der Swaluw et al. 2004). The interaction also temporarily increases the magnetic field, causing a rapid burn-off of the highest energy particles and enhanced synchrotron emission. When the reverse shock passes the pulsar itself, it sweeps the nebula along with it, pro-

ducing a relic PWN composed of low energy particles, typically observed at radio wavelengths (e.g., Temim et al. 2013). The pulsar's continued injection of fresh high-energy particles forms a new X-ray PWN that is now displaced from the radio relic. There is typically a trail of X-ray emission connecting the pulsar to the radio PWN that may show evidence for spectral steepening due to synchrotron aging of particles as they travel away from the pulsar.

A fascinating example of an aged composite SNR that exhibits virtually all of the properties described above is SNR G327.1-1.1 (Temim et al. 2009, 2015). A deep 350 ks ACIS-I observation, shown in Fig. 7, reveals the elaborate morphology of a PWN formed by a rapidly moving pulsar that has fully been disrupted by the SN reverse shock. A narrow trail of emission connects the X-ray nebula to a radio relic PWN that is significantly displaced from the center of the surrounding SNR shell (see Fig. 8). The presumed pulsar is identified by *Chandra* as a point source embedded in a cometary X-ray nebula, with a pair of narrow prong-like structures protruding towards the NW, and extending into more diffuse, large arcs. There is also evidence for mixing of SN ejecta with the PWN material that is
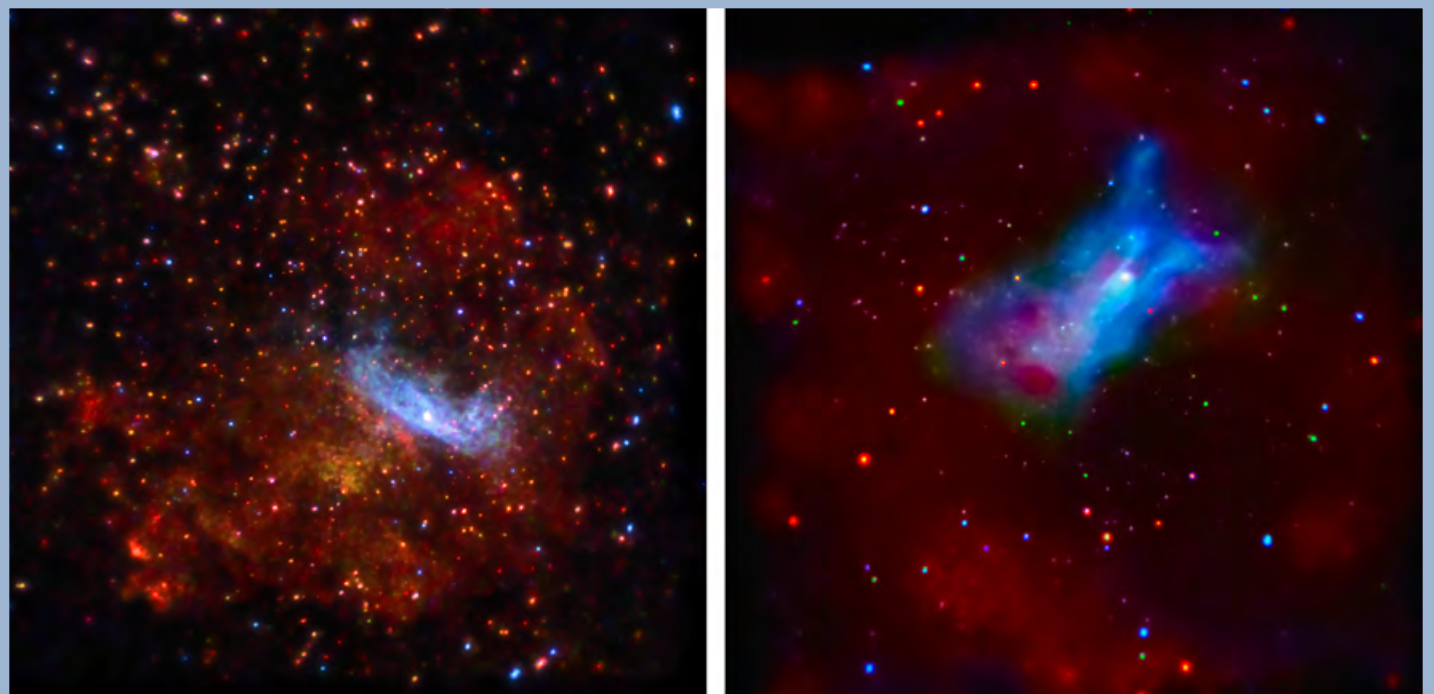

Fig. 7 — Chandra press release images of two composite SNRs in different stages of evolution with the 0.75–1.45 keV emission in red, 1.45–2.58 keV emission in green, and 2.58–7.0 keV emission in blue. Left: Intermediate age SNR MSH 11-62 (Slane et al. 2012), showing an asymmetric PWN located off-center of the thermal shell of its host SNR. The morphology suggests that the PWN is being compressed by the SN reverse shock. Right: A highly evolved composite SNR G327.1-1.1 (Temim et al. 2015) showing a faint thermal shell (red) and a PWN produced by a rapidly moving pulsar that has already been completely disrupted by the SN reverse shock. The thermal emission observed in the PWN region (red colored region in the center) is indicative of mixing of SN ejecta with PWN material.
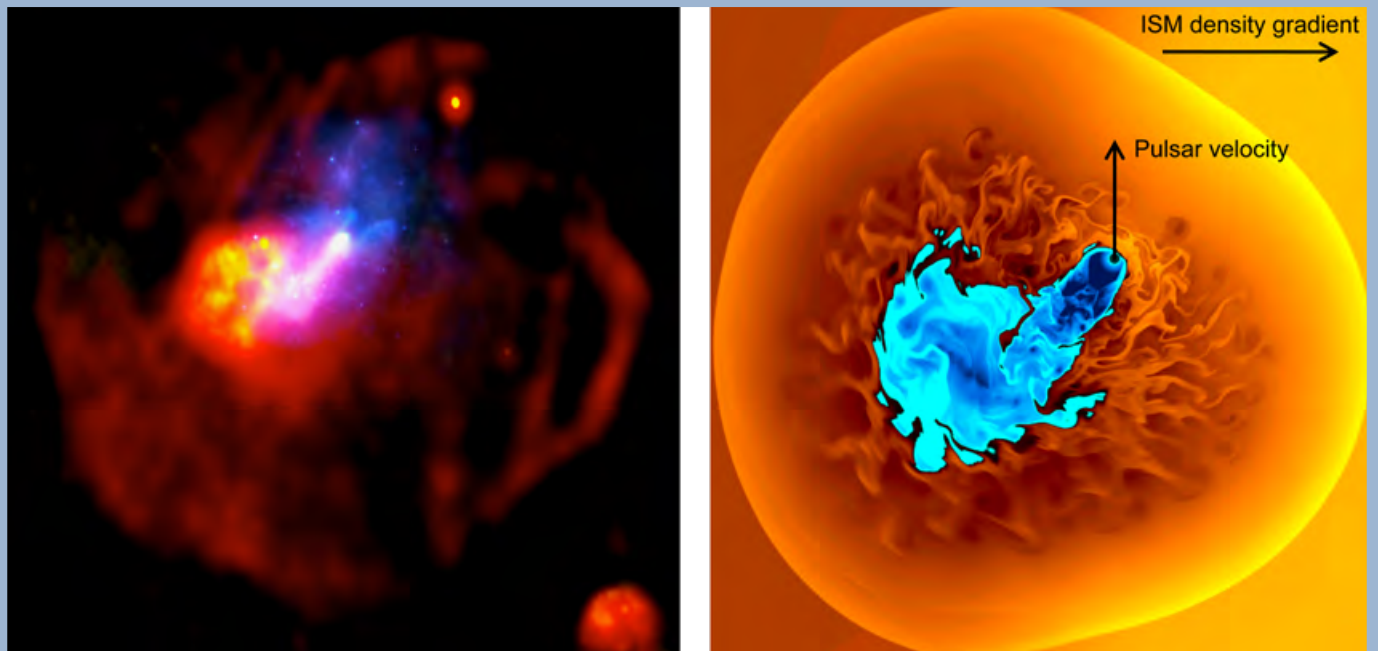
Fig. 8 — Left: Evolved composite SNR G327.1-1.1 with radio emission shown in red and Chandra X-ray emission in blue (Temim et al. 2009). The PWN seen in the radio is the relic nebula that was swept away from the pulsar by the SN reverse shock. Chandra revealed a newly-forming X-ray nebula with a cometary structure and a trail of emission connecting it back to the radio relic. A curious outflow of PWN material is seen ahead of the pulsar towards the NW. Right: A density map from an HD simulation of G327.1-1.1 constrained by the properties derived from the Chandra observation (Temim et al. 2015); an average density of 0.12 cm^{-3}, an SNR (PWN) radius of 22 pc (5 pc), a PWN luminosity of 7×10^{34} erg s^{-1}, a pulsar velocity of 400 km s^{-1}, and an SNR age of 17,000 yr. In the simulation, the ISM density gradient increases from east to west, and the pulsar moves to the north. This causes the reverse shock to arrive preferentially from the NW, displacing the bulk of the PWN material in this direction. The resulting morphology is remarkably similar to the radio and X-ray observations of the SNR.

expected to result from a reverse shock interaction. Furthermore, this SNR is a confirmed source of γ-ray emission that likely arises from the PWN (Acero et al. 2012).

Exciting new progress has been made in understanding these various structures through HD modeling of composite SNRs expanding in a non-uniform ISM and hosting a rapidly moving pulsar. An HD simulation of G327.1-1.1 (Fig. 8), constrained by the observationally determined SNR and PWN properties, reproduced the morphology of the SNR remarkably well (Temim et al. 2015). The observed properties can be explained by a scenario in which the ambient density gradient decreases from west to east, and the pulsar moves to the north with a velocity 400 km s^{-1}, causing the reverse shock to crush the PWN preferentially from the NW direction. The model implies that the SNR's morphology most strongly depends on the strength and orientation of the ISM density gradient, and the pulsar's velocity, spin-down luminosity, and spin-down timescale. It also allows us to place constraints on the SN ejecta mass (~ 4.5 M$_\odot$ in this case), and predict the spectral steepening expected from synchro-

tron cooling, that can be compared with observations. Using these same physical parameters, a semi-analytical model for composite SNR evolution (Gelfand et al. 2009) reproduces the broadband spectrum of the PWN at radio, X-ray, and γ-ray bands. The model implies an electron spectrum with a break at 300 GeV, corresponding to a spectral break in the mid-infrared (Temim et al. 2015). The self-consistent evolutionary model for the morphology and broadband emission of G327.1-1.1 demonstrates the power of modeling of composite SNRs whose properties can at least partially be constrained by observations.

Future Prospects

This review highlighted only a selection of recent studies, focusing on Type Ia SNRs and three special classes of CC SNRs; those that interact with molecular clouds, those that likely originate from bipolar or jet-driven explosions, and composite SNRs that contain a PWN. Future studies with *Chandra* will certainly further increase our knowledge about these systems and provide insight into many of the outstanding questions.

Chandra will potentially identify other prospects for Type Ia SNRs that have CSM interactions, particularly in coordination with HD simulations. Its longevity has a serendipitous effect in that the baseline for proper motion studies only grows longer. Older measurements can be refined and new expansion measurements can be made for the first time, even for more distant SNRs.

Chandra and *XMM-Newton* will be necessary to spatially resolve the overionized plasma and ascertain the cause of the rapid electron cooling in interacting SNRs. Future kinematic studies can confirm the bipolar nature of some SNRs, as it is predicted that heavy metals (Cr, Mn, Fe) should have faster velocities than lighter elements (O, Mg, Si). Additionally, improved measurements of chemical abundances via X-ray spectroscopy may better constrain parameters like the progenitor mass, the explosion energy, and the jet opening angle.

Future modeling of composite SNRs in different evolutionary stages promises to further improve our understanding of the PWN/SNR interaction, constrain parameters such as the pulsar's spin-down timescale and the SN ejecta mass, and help uncover the eventual fate of accelerated particles that escape into the ISM. The models will hinge on high-resolution observational studies with *Chandra* that can constrain the PWN structure, spatial variations in the PWN spectrum, and the properties of the SNR thermal emission.

The fifteen years of *Chandra* observations have led to extraordinary advances in our understanding of the evolution of SNRs and the origin of their diversity. The next fifteen years hold the promise of many more great discoveries.

Acknowledgments

References

Acero, F., Djannati-Ataï, A., Förster, A., et al. 2012, arXiv:1201.0481.

Abdo, A. A., Ackermann, M., Ajello, M., et al. 2010, ApJ, 713, 146.

Badenes, C., et al. 2007, ApJ, 662, 472.

Bhalerao, J., Park, S., Dewey, D., et al. 2015, ApJ, 800, 65.

Blondin, J. M., Chevalier, R. A., & Frierson, D. M. 2001, ApJ, 563, 806.

Bocchino, F., van der Swaluw, E., Chevalier, R., & Bandiera, R. 2005, A&A, 442, 539

Borkowski, K. J., et al. 2013, ApJ, 771, 9.

Borkowski, K. J., et al. 2014, ApJ, 790, 18.

Burkey, M. T., et al. 2013, ApJ, 764, 63.

Chiotellis, A., et al. 2012, A&A, 537, 139.

Cox, D. P, et al. 1999, ApJ, 524, 179.

Eriksen, K. A., et al. 2011, ApJ, 728, 28.

Fruchter, A. S., et al. 2006, Nature, 441, 463.

Gaensler, B. M., & Wallace, B. J. 2003, ApJ, 594, 326.

Gilfanov, M. & Bogdan, A. 2010, Nature, 463, 924.

Hughes, J. P., et al. 2000, ApJL, 528, L109.

Hughes, J. P., Slane, P. O., Burrows, D. N., et al. 2001, ApJL, 559, L153.

Itoh, H. & Masai, K. 1989, MNRAS, 236, 885.

Izzard, R. G., et al. 2004, MNRAS, 348, 1215.

Kawasaki, M. et al. 2005, ApJ, 631, 935.

Kaspi, V. M., Roberts, M. E., Vasisht, G., et al. 2001, ApJ, 560, 371.

Katsuda, S., et al. 2013, ApJ, 763, 85.

Matheson, H., & Safi-Harb, S. 2010, ApJ, 724, 572.

Lopez, L., et al. 2009, ApJ, 706, 106.

Lopez, L., et al. 2011, ApJ, 732, 114.

Lopez, L., et al. 2013a, ApJ, 777, 145.

Lopez, L., et al. 2013b, ApJ, 764, 50.

Lopez, L., et al. 2014, ApJ, 777, 5.

Maeda, K. & Nomoto, K. 2003, ApJ, 598, 1163.

Ozawa, M. et al. 2009, ApJL, 706, L71.

Park, S., Hughes, J. P., Slane, P. O., et al. 2007, ApJ, 670, L121.

Patnaude, D. J., et al. 2012, ApJ, 756, 6.

Peters et al. 2013, ApJL, 771, L38.

Ramirez-Ruiz & MacFadyen 2010, ApJ, 716, 1028.

Reynolds, S.P., et al. 2007, ApJ, 668, 135.

Reynolds, S.P., et al. 2008, ApJ, 680, 41.

Roberts, M. S. E., Tam, C. R., Kaspi, V. M., et al. 2003, ApJ, 588, 992.

Safi-Harb, S., Harrus, I. M., Petre, R., et al. 2001, ApJ, 561, 308.

Sanders, N. E., et al. 2012, ApJ, 758, 132.

Seitenzahl, I. R., et al. 2013, MNRAS, 429, 1156.

Soderberg, A., et al. 2010, Nature, 463, 513.

Slane, P., Castro, D., Funk, S., et al. 2010, ApJ, 720, 266.

Slane, P., Chen, Y., Schulz, N. S., et al. 2000, ApJ, 533, L29.

Slane, P., Hughes, J. P., Temim, T., et al. 2012, ApJ, 749, 131.

Temim, T., Slane, P., Castro, D., et al. 2013, ApJ, 768, 61.

Temim, T., Slane, P., Gaensler, B. M., Hughes, J. P., & Van Der Swaluw, E. 2009, ApJ, 691, 895.

Temim, T, et al. 2015, ApJ, submitted.

Uchida, H., et al. 2013, ApJ, 771, 56.

van der Swaluw, E., Downes, T. P., & Keegan, R. 2004, A&A, 420, 937.

Vink, J. 2012, A&AR, 20, 49.

Wang, L. & Wheeler, C. J. 2008, ARA&A, 46, 433.

Wardle, M. & Yusef-Zadeh, F. 2002, Science, 296, 2350.

Williams, B.J., et al. 2012, ApJ, 755, 3.

Winkler, P.F., et al. 2013, ApJ, 764, 156.

Winkler, P.F., et al. 2014, ApJ, 781, 65.

Yamaguchi, H., et al. 2009, ApJL, 705, L6.

Zajczyk, A., Gallant, Y. A., Slane, P., et al. 2012, A&A, 542, A12.